Microgel Formation and Thermo-Mechanical Properties of UV-Curing Unsaturated Polyester Acrylates

Ahmet Nebioglu, Mark D. Soucek

Department of Polymer Engineering, The University of Akron, Akron, Ohio 44325

Received 16 May 2006; accepted 1 June 2007
DOI 10.1002/app.27381
Published online 9 November 2007 in Wiley InterScience (www.interscience.wiley.com).

ABSTRACT: The effect of internal and terminal unsaturation on the properties of the acrylated polyester films was investigated. Four types of acrylated polyester resin were prepared using adipic acid, maleic anhydride, neopentyl glycol, trimethylolpropane, and acrylic acid. Terminal and internal double bond content as well as branching was adjusted by the molar quantities of trimethylolpropane and maleic anhydride, respectively. A reactive diluent, trimethylolpropane triacrylate (TMPTA), was also used. A three-factor, three-level Box-Behnken design was used to investigate complex nonlinear relationships. Dynamic mechanical, fracture toughness, and tensile properties were evaluated with respect to the amount of terminal and internal unsaturation, and reactive diluent concentration. It was found that microgel formation extensively affects the final UV-cured film properties. Small quantities of microgels function as micro-support units, whereas high extent of microgelation causes phase separation through cluster formation and hence, decreases the mechanical properties. It is essential to control the extent of microgelation and phase separation to optimize product performance. © 2007 Wiley Periodicals, Inc. J Appl Polym Sci 107: 2364–2374, 2008

Key words: polyesters; photopolymerization; viscoelastic properties; thin films; microgel

INTRODUCTION

Unsaturated polyesters (UPEs) are one of the most widely used resins for glass-reinforced composites. In wood finishing, UPEs are utilized as fillers, sealers, and topcoats.[1] A typical polycondensation technique can be used to carry-out the reaction of diacids, one of which is typically maleic anhydride, with glycols.[2] Styrene is usually incorporated into the coating formulations as a reactive diluent to reduce viscosity, increase the crosslink density, and decrease cost.[3] In terms of pot-life stability, it is necessary to use radical scavengers to inhibit polymerization of the carbon–carbon double bonds. Replacement of the volatile styrene monomer with higher molecular weight and functionality reactive diluents is necessary to obtain higher throughput, reactivity, mechanical properties, and moreover reduce odor.[4]

There are two methods to cure UPEs: conventionally by initiation with an organic peroxide[5] and photochemically by using a photoinitiator.[6] The photochemical UV-curing process has the advantages of shorter cure times, reduced solvent emission, and lower overall cost. Current UV-cure coatings are predominantly based on acrylated oligomers due to their relatively higher reactivity and lower volatility. Polyester acrylates are prepared through the reaction of either the hydroxyl terminated polyesters with acrylic acid or the carboxyl terminated polyesters with hydroxyethyl acrylate.[3]

Mechanical and viscoelastic properties of the UPEs are greatly affected by the network structure of the crosslinked polymer.[3] Possible free radical curing mechanisms of UPEs consist of both intra- and intermolecular reactions.[7] Intramolecular reactions result in cyclization and formation of microgel structures through encapsulation of reactive monomers and oligomers as shown in Figure 1.[8–11] As the curing proceeds further, concentration of the microgels increases, causing crosslinking between microgels, and finally the macrogelation.

Heterogeneous crosslinking mechanism and network structure of conventionally curing UPE/styrene,[12] vinyl ester/styrene,[13] and acrylate[14,15] systems were studied extensively. Microgel formations were verified for these systems using various characterization techniques including dynamic mechanical thermal analyzer (DMTA), atomic force microscopy (AFM), and dynamic light scattering (DLS). Effects of terminal acrylate unsaturation on the rheological behavior of the thermally cured UPE/styrene system were earlier studied by Djonlagic and coworkers.[16–18] It was concluded that introduction of terminal acrylate groups decreases the number of dangling chains and therefore allows the formation of

Correspondence to: M. D. Soucek (msoucek@uakron.edu).

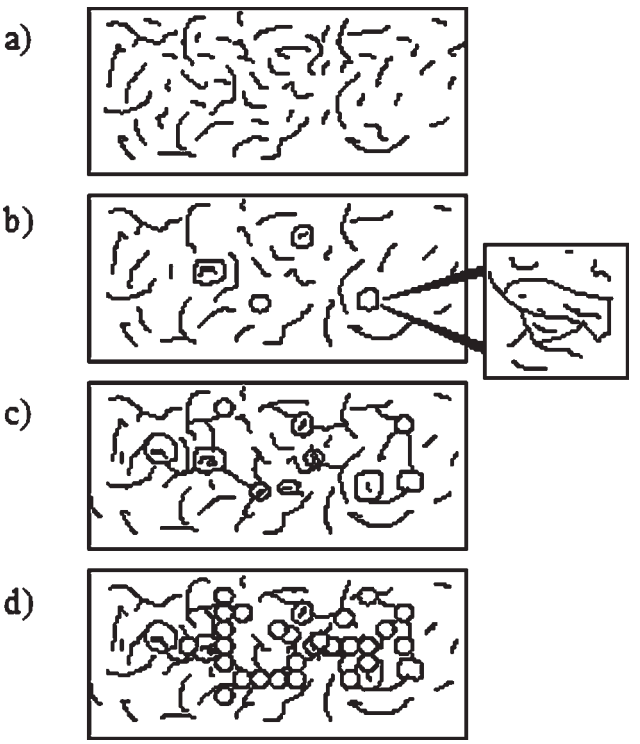

Figure 1 Heterogeneous curing mechanism of UPEs: (a) beginning of curing; (b) microgel formation; (c) crosslinking between microgels; (d) macrogelation.

more regular networks. The UV-free radical polymerization of multifunctional acrylates also leads to the formation of heterogeneous networks through generation of microgels.[19–21] Barbeau et al. proposed a ''spider-web'' like network structure, and explained it through the development of microgel clusters connected by polyacrylate and soft polyether chains.[22]

There is, however a deficiency in the literature in understanding and optimization of free radical UV-cured unsaturated polyester acrylate resins. While there has been a plethora of work on UPE with monofunctional reactive diluent systems, no studies thus far have been reported on the effect of location of the unsaturation in UPE resins utilizing multifunctional reactive diluent on the final film properties. The aim of this study is to investigate effect of the concentration of the reactive multifunctional monomer and terminal acrylate unsaturation in UV-curing unsaturated polyester acrylate coatings. For this purpose, unsaturated polyester acrylates containing varying levels of unsaturation and acrylate functionality synthesized. Design of experiments (DOE) was utilized to observe complex structure–property relationships and quantify interaction of two or more factors.[23,24] It was possible to obtain nonlinear relationships which could not be derived from simple experiments. As the variables acrylate functionality, internal unsaturation and reactive diluent concentration changed and dynamic mechanical, fracture toughness, tensile, reverse impact resistance response data were observed. Four different types of polyester acrylates out of several possibilities were depicted in Scheme 1.

EXPERIMENTAL

Materials

Monomers to prepare unsaturated polyester acrylates; adipic acid (ADA), trimethylol propane (TMP), and neopentyl glycol (NPG), were purchased from Aldrich. Photoinitiator, 1-hydoxy-cyclohexyl-phenyl-ketone (IRGACURE 184) was obtained from Ciba Specialty Chemicals. Reactive diluent (trimethylolpropane triacrylate, TMPTA), esterification

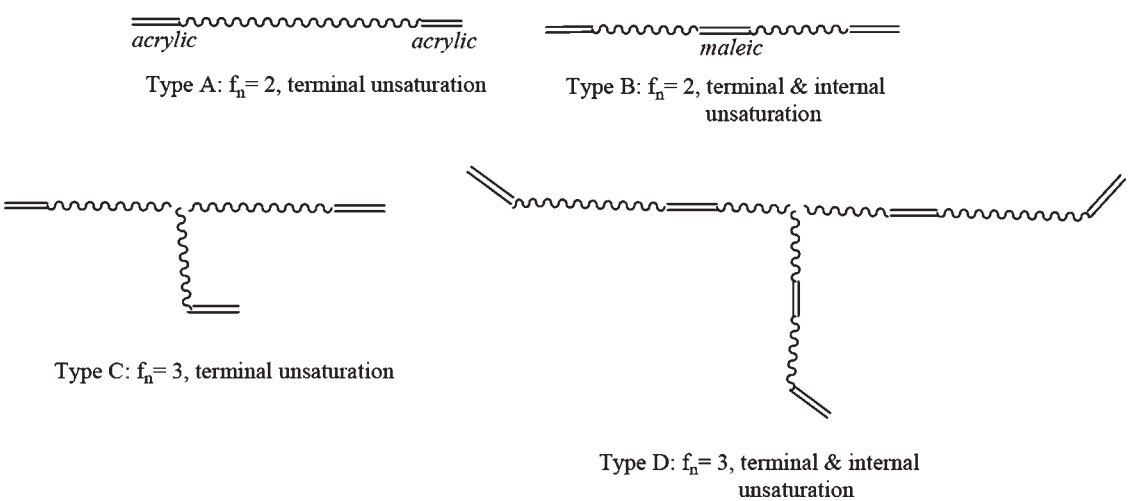

Scheme 1 Possible polyester types with different unsaturations and functionalities.

catalysts (dibutyltinoxide, *para*-toluenesulphonic acid), and inhibitor (hydroquinone) were also purchased from Aldrich. A wetting agent, Tegowet 270 supplied from Degussa Corporation. All the materials were used as received without any purification. The chemical structures of the monomers, reactive diluent, and the photoinitiator are shown in Scheme 2.

Preparation of the polyesters

Different types of polyesters were prepared in terms of internal unsaturation content and acrylate functionality by varying MA and AA molar amounts used in the synthesis. For all of the resins, hydroxyl functional polyesters containing different amounts of MA were synthesized via a two stage polycondensation technique to avoid gel formation,[25] and then reacted with AA. Quantities of the monomers used in the synthesis were determined according to the Box–Behnken DOE to give various functionality and internal unsaturation. For the first stage, ADA, MA, and NPG were reacted at 185°C for 3.5 h ''with a 2 : 1; diacid : diol ratio.'' In the second stage, the remaining polyol (NPG or TMP) was added to the reaction flask to obtain a total diacid : polyol molar ratio 2 : 3. Temperature of the flask was kept at 185°C for 2 h 20 min and then increased to 210°C. As the catalyst, 0.3% dibutyltinoxide was utilized. The reaction was performed in a three-necked flask equipped with a mechanical stirrer and Dean-Stark trap under a nitrogen purge until the resultant polyester resin had an acid value of 10 mg KOH/g (ASTM D 1639-90). Amount of each monomer used, and functionality (f_n), number average molecular weight, and polydispersity of the polyester resins prepared are listed in Table I.

The polyesters were characterized by Fourier transform-infrared (FTIR), nuclear magnetic resonance (NMR) spectroscopy, and gel permeation chromatography (GPC). Hydroxyl functionalities of the polyesters were acrylated via using acrylic acid (AA) at 115°C for 12 h. Molar amount of acrylic acid was 1.1 × (hydroxyl equivalent number of the polyester). About 0.3 wt % *p*-toluenesulphonic acid (*p*-TSA) and 0.1 wt % hydroquinone were used as the catalyst and the inhibitor, respectively. Excess AA was removed *in vacuo* at 100°C. Yield of the acrylation reactions were determined to be 90% ± 1% using ^{1}H NMR spectrometry.

Formulations and film formation

The coating formulations were prepared according to the Box–Behnken response surface design lattice[23,24] given in Figure 2. Factors (TMP, MA, and TMPTA) and their levels were summarized in Table II. Functionality and the internal unsaturation content of the polyester resins are adjusted by changing the amount of TMP and MA, respectively during the synthesis of the polyester resins shown in Table I.

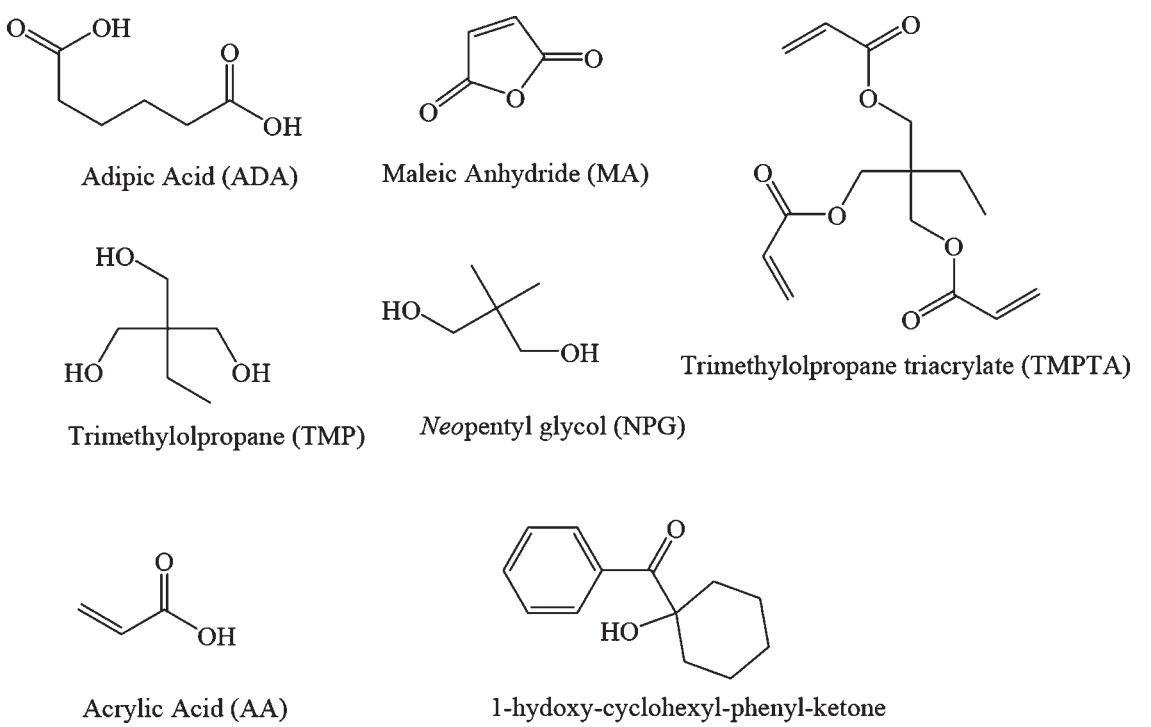

Scheme 2 Structures of the monomers, reactive diluent, and the photoinitiator.

TABLE I
Monomer Amounts Used and the Properties of the Polyester Resins

	1st Stage				2nd Stage				
Resin	ADA[a]	NPG[a]	TMP[a]	MA[a]	NPG[a]	TMP[a]	f_n	$\overline{M}_n$	$\overline{M}_w/\overline{M}_n$
m0-f2[b]	2	1	0	0	2	0	2	800	1.3
m0-f2.5	2	1	0	0	1.5	0.5	2.5	900	1.3
m0-f3	2	1	0	0	1	1	3	900	1.4
m0.5-f2	1.5	1	0	0.5	1	0	2	800	1.3
m0.5-f2.5	1.5	1	0	0.5	1.5	0.5	2.5	800	1.4
m0.5-f3	1.5	1	0	0.5	1	1	3	900	1.4
m1-f2	1	1	0	1	2	0	2	1000	1.3
m1-f2.5	1	1	0	1	1.5	0.5	2.5	800	1.4
m1-f3	1	1	0	1	1	1	3	1000	1.4

[a] All the monomer amount units are in moles.
[b] m0 and f2 denotes MA content (0) and hydroxyl functionality (2) of the corresponding polyester resin.

As the reactive diluent, TMPTA was used to obtain good crosslink densities and rigid films. A unimolecular photoinitiator (Irgacure 184), 4% of the total amount of TMPTA and acrylated polyester, incorporated into the formulations for UV-curing. A wetting agent, Tegowet 270, 1% of the total formulation, was added to the coating formulations to adjust the surface tension and obtain crater-free films. The coatings were casted on aluminum and glass panels by a draw-down bar with a thickness of 130 μm. The thin wet films were cured in a UV-processor for 0.1 min with two different intensities, measured by UV Power Pluck Radiometer (EIC), given in Table III. If otherwise was not mentioned, the UV-curing intensity was ''intensity-1.''

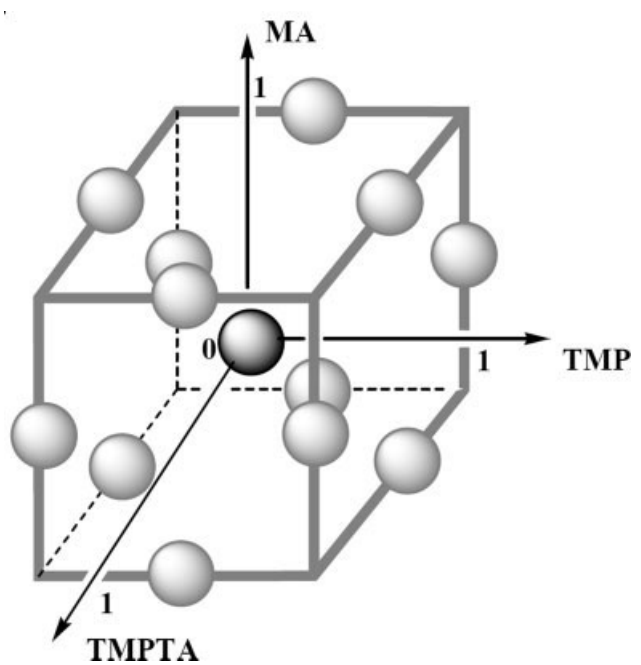

Figure 2 Box–Behnken Design Lattice.

Instrumentation

The viscoelastic properties were measured on a dynamical mechanical thermal analyzer (DMTA V, Rheometrics Scientific) with a frequency of 1 Hz and a heating rate of 4°C/min over a range of −100 to 200°C. The gap distance was set up at 5 mm for rectangular test specimens (length 10 mm, width 5 mm and thickness 0.06–0.10 mm). Tensile tests were performed on an Instron 5567 (Instron Corporation). Reverse impact resistance (ASTM 2794-84) was measured according to ASTM standards.

FTIR spectra were obtained on a Mattson Genesis Series FTIR. ^{1}H NMR spectra were recorded on a Gemini-300 spectrometer (Varian) in $CDCl_3$ solvent with tetramethylsilane (TMS) as a reference. A Waters GPC system with a HR4, HT2, HR1, HR0.5 Styragel, and 500 Å Ultrastyragel columns connected in series were used to characterize the polyesters. Tetrahydrofuran was applied as the mobile phase and delivered at a rate of 1.0 mL/min. The thin wet films were cured in a Fusion F300 UV-processor (H-bulb; Fusion UV system).

Plane-stress fracture toughness measurements were conducted on rectangular specimens with single-edge-notch geometry. The dimensions of the films were 10.2 mm × 11.0 mm × 0.06–0.10 mm (width ×

TABLE II
Factors and their Levels for Box–Behnken Response Surface Design

	Level		
Factors	−1	0	1
A: TMP (moles)[a]	0	0.5	1
B: MA (moles)[a]	0	0.5	1
C: TMPTA (%)[b]	20	35	50

[a] In 5 mol polyester resin.
[b] Based on the amount of the polyester resin.

TABLE III
UV-Light Intensities Used to Cure Coating Formulations

	Intensity-1 (W/cm^2)	Intensity-2 (W/cm^2)
UVA 320–390 nm	2.0	1.3
UVB 280–320 nm	1.5	1.0
UVC 250–260 nm	0.18	0.12
UVV 395–445 nm	1.3	0.81

length × thickness). Each film was cut with a razor blade to create the edge notch. The length of the notch was less than 10% of the width of the sample. A fracture toughness tester which was mounted on a microscope stage and equipped with a 25 lb_f load cell and a variable speed motor was used to deform the specimen in a tensile mode. The crosshead speed was 0.583 mm/min. The load displacement curve was digitally recorded by a computer. The crack tip region was observed at a magnification of 100× on the computer monitor, and the onset of crack propagation was noted and digitally marked on the load displacement curve. The deformation zone near the crack tip could be observed continuously on the computer monitor during the loading. Six samples were tested for each film. The data are reported as the mean of the data set. The plane-stress fracture toughness (K_c, stress intensity factor at fracture) was calculated using eq. (1),[26,27]

$$K_c = \left[3.94\left(\frac{2w}{\pi a}\right)\tan\left(\frac{\pi a}{2w}\right)\right]^{1/2}\frac{F}{(w-a)b}\sqrt{a} \qquad (1)$$

where w is the width, a is the notch length, b is the thickness, and F is the force at which crack propagation begins.

RESULTS AND DISCUSSION

Understanding, modeling, and characterization of the free radically UV-cured UPE acrylate-reactive monomer networks is essential to optimize the product performance. Although UPEs have relatively slow UV-curing rates compared with acrylated polyesters, UPEs are more cost-effective.[3] Therefore, with using UPE acrylates it may be possible to obtain a faster curing, lower cost, and higher performance films or composite matrix. In this study, thermomechanical properties of the UV-curing internal and terminal unsaturated polyesters were compared. Extent of internal and terminal unsaturation is controlled by adjusting maleic anhydride content and branching of the polyesters, respectively.

A DOE methodology was employed before the preparation of the resins and formulations to depict complex material properties. A three-factor, three-level Box–Behnken design is one of many response surface designs used to construct the response surface for the analysis and optimization of the coatings formulations. It is chosen due to its ability to effectively model the design space with relatively low number of experiments. Design Expert software (Stat-Ease, Minneapolis, MN) was used to obtain the statistical modeling of the design space. Fracture toughness, tensile strength, and reverse impact resistance tests were selected to elucidate the balance of mechanical properties.

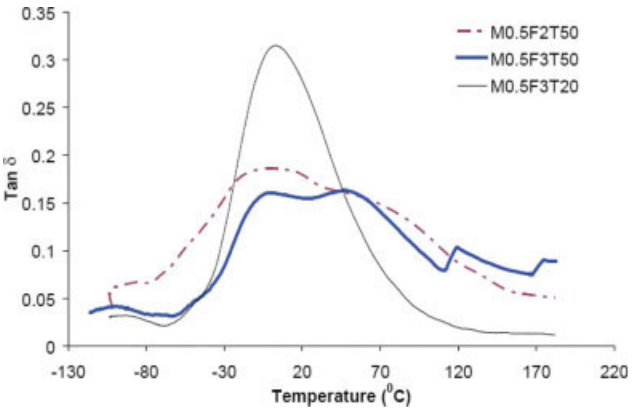

Figure 3 Tan δ behavior of the UV-cured films with different functionalities and reactive diluent content. [Color figure can be viewed in the online issue, which is available at www.interscience.wiley.com.]

The viscoelastic properties of the films were measured using a DMTA. Loss factor, tan δ behavior of the coatings is shown in Figures 3–5. The high reactive diluent (TMPTA) concentrations resulted in phase separated films indicated by the two transitions in tan δ graphs (see Fig. 3). Increase of the acrylate functionality caused more distinct transition maximums. Addition of internal unsaturation via MA also resulted in two tan δ transitions (see Fig. 4, M1F2T35, M1F3T35), and therefore phase separation.

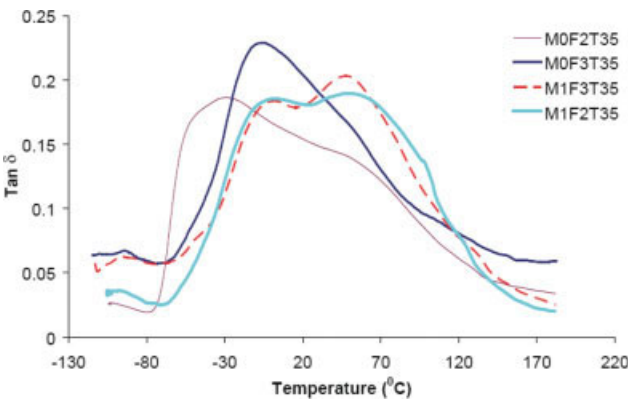

Figure 4 Tan δ behavior of the UV-cured films with different functionalities and internal unsaturation content. [Color figure can be viewed in the online issue, which is available at www.interscience.wiley.com.]

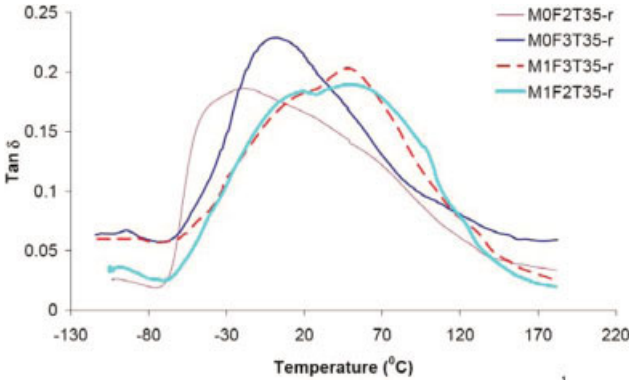

Figure 5 Tan δ behavior of the UV-cured films during the 2nd DMTA analyses. [Color figure can be viewed in the online issue, which is available at www.interscience.wiley.com.]

When the samples were reanalyzed from −100 to 200°C, all the tan δ transitions shifted to higher temperatures and fusion of the transition maximums observed. The storage modulus (E') showed a slightly decreasing trend until temperature reached −50°C. Between −50 and 50°C, E' decreased dramatically for all the films. The crosslink density of the films was calculated from the eq. (2).[28]

$$E'(\min) = 3\nu_e RT \quad (T \gg T_g) \tag{2}$$

where, ν_e is the number of moles of elastically effective chains per cubic centimeter of the film, E' (min) is the minimum storage modulus in the rubbery plateau. The E' (min), crosslink density (ν_e), and breadth of tan δ transition of the polyester acrylate films are listed in Table IV.

TABLE IV
Viscoelastic Properties of the UV-Cured Polyester Films

	E' (min) (N/m^2)	Crosslink density (mol/cm^3)	Tan δ breadth[a] (°C)
M0.5F2T50[b]	2.68×10^7	2.66×10^{-3}	150
M0.5F3T50	2.32×10^7	2.48×10^{-3}	153
M0.5F3T20	1.60×10^7	1.40×10^{-3}	71
M0F2T35	2.29×10^7	2.02×10^{-3}	148
M0F3T35	3.57×10^7	3.54×10^{-3}	96.9
M1F3T35	2.98×10^7	2.94×10^{-3}	126
M1F2T35	2.90×10^7	2.57×10^{-3}	141
M0F2T35-r[c]	2.77×10^7	2.52×10^{-3}	141
M0F3T35-r	3.78×10^7	3.90×10^{-3}	93.0
M1F3T35-r	3.90×10^7	4.12×10^{-3}	120
M1F2T35-r	3.22×10^7	3.01×10^{-3}	138

[a] Width at half height of tan δ.
[b] M0.5F2T50 denotes the film formed through the polyester resin m0.5f2 with 50% TMPTA based on the amount of the polyester resin.
[c] "r" denotes the reanalyzed samples.

As the extent of internal and terminal unsaturation was increased one would expect an increase in crosslink density. This was not always case. The only difference between M0.5F2T50-M0.5F3T50 and M1F3T35-M0F3T35 is the acrylate-functionality and MA content respectively. It can be expected that M0.5F2T50 would have significantly lower crosslink density than M0.5F3T50 due to its lower acrylate functionality. Similarly, M0F3T35 would have lower crosslink density than M1F3T35, as M0F2T35 has lower crosslink density with respect to M0F3T35 or M1F2T35. However, crosslink density data calculated via DMTA (see Table IV) revealed that M0F3T35 (3.54×10^{-3} mol/cm^3) and M0.5F2T50 (2.66×10^{-3}) had higher crosslink density than M1F3T35 (2.94×10^{-3}) and M0.5F3T50 (2.48×10^{-3}), respectively. After a second DMTA run, however, the crosslink density order was adjusted to the expected values i.e. according to the amount of the double bond concentration of the resins.

The most feasible explanation for the initial diminution crosslink density behavior is the trapping of free radicals, as in UPE/styrene system.[29] It was reported that free radical were trapped inside the microgels due to the intramolecular cyclization reactions as shown in Figure 6. The higher acrylate-functionality content causes more microgelation, more trapped radicals, and therefore lower crosslink density for either high concentrations of multifunctional monomer (TMPTA) or internal unsaturation (MA). Similarly, higher MA content also causes more microgels. It is also evident that during the first DMTA thermogram, at elevated temperatures trapped free radicals mobilize and start reacting inside the microgels. After cooling, the second thermogram resulted in films having more complete reactions and, thus higher crosslink densities.

The breadth of the α-transition was independent of the crosslink density (see Table IV). The breadth of a transition region is closely related to the degree of heterogeneity[30] and higher crosslink densities do not necessarily cause more heterogeneous systems. Heterogeneity was affected by the extent of polyester-acrylate functionality, internal unsaturation (MA), and multifunctional reactive diluent

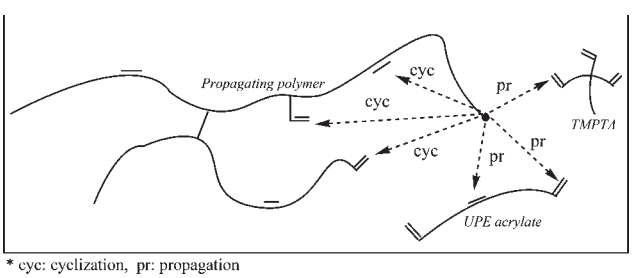

Figure 6 Possible reactions of a growing chain.

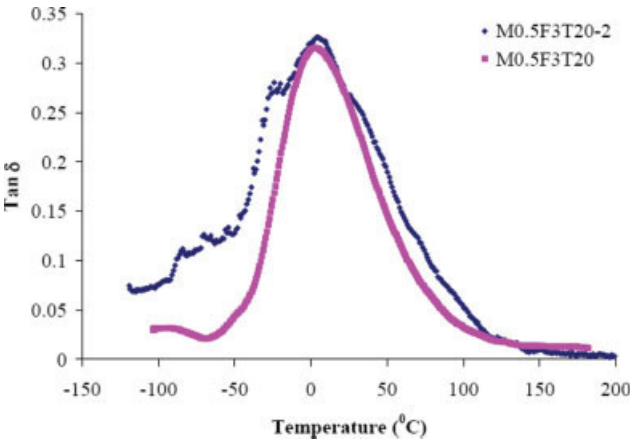

Figure 7 Tan δ behavior of M0F3T20 at two different UV-intensities. [Color figure can be viewed in the online issue, which is available at www.interscience.wiley.com.]

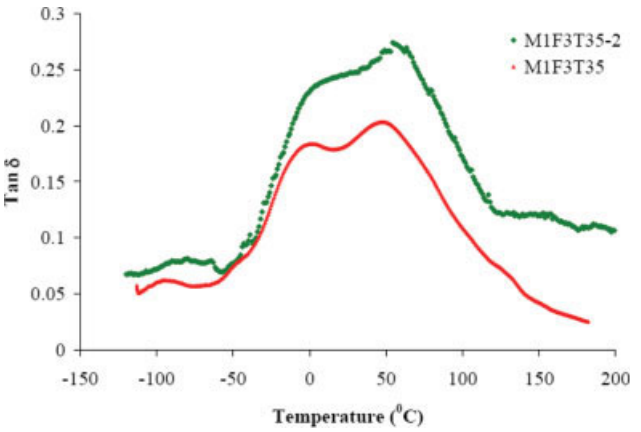

Figure 9 Tan δ behavior of M1F3T35 at two different UV-intensities. [Color figure can be viewed in the online issue, which is available at www.interscience.wiley.com.]

(TMPTA). The least and the most heterogeneous films were the ones containing lowest and highest amounts of TMPTA (M0.5F3T20, M0.5F3T50), therefore multifunctional monomer is the variable which has the highest impact on the heterogeneity. After the second (repeat) DMTA thermogram, the breadth of tan δ decreased slightly due to further reactions of the trapped free radicals in the microgel regions.

Comparison of the tan δ behavior of the films cured at different UV-intensities given in Table III was depicted in Figures 7–9. High intensity cured film containing moderate level of MA and low level of TMPTA (M0.5F3T20) exhibited just a single tan δ transition, whereas low intensity cured film (M0.5F3T20-2) had an extra shoulder and a broader peak. Lower intensity cured film based on the resins having three acrylate functionality, moderate level of TMPTA, and no MA (M0F3T35-2) showed a higher temperature second tan δ transition maxima. Curing at lower UV-intensity also resulted in overall tan δ transition shift to the higher temperatures. Similar right shift of tan δ was also observed with the high MA containing resins (M1F3T35, M1F3T35-2). These results indicate more heterogeneous and higher T_g films with lower UV-intensity cured films. Formation of the shoulders or second peak maximums implies phase separation with low intensity cure. As the UV-intensity was reduced, energy and hence amount of photons starting the photoinitiator dissociation reaction decreases. This allows more time for microgel and a microgel-rich high T_g phase formation.

Crosslink density behaviors listed in Table V support the formation of more microgels, as low intensity cured films had lower crosslink densities. Secondary relaxation processes or β-transitions involve fewer carbon atoms and demonstrates more localized motions compared with α- transitions. The β-transitions have been assigned to the onset of motions prior to the long range segmental motions occurring at glass transition. However, β-relaxations are not always detectable.[31] Fracture toughness, tensile

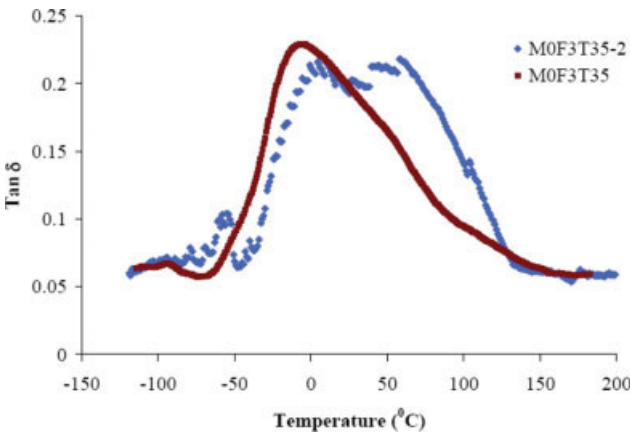

Figure 8 Tan δ behavior of M0F3T35 at two different UV-intensities. [Color figure can be viewed in the online issue, which is available at www.interscience.wiley.com.]

TABLE V
Properties of Low and High UV-Intensity Cured Films

	Tensile strength (MPa)	K_c MPa.m$^{0.5}$	Impact resistance (kg/cm)	Crosslink density (mol/cm^3)
M0.5F3T20	4.0	43	32	1.40×10^{-3}
M0.5F3T20-2	3.5	48	45	1.22×10^{-3}
M0F3T35	5.6	55	5.3	3.54×10^{-3}
M0F3T35-2	4.5	60	21	1.35×10^{-3}
M1F3T35	7.0	98	12	2.94×10^{-3}
M1F3T35-2	7.5	101	24	1.51×10^{-3}

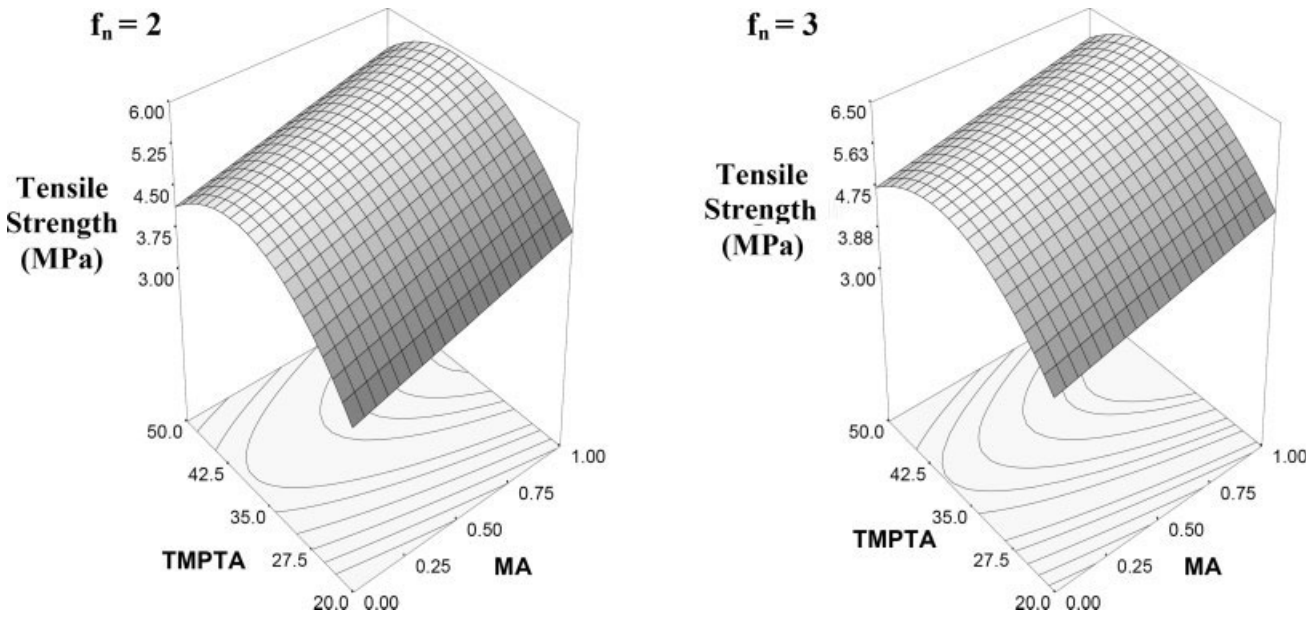

Figure 10 Tensile strength 3D response surface graphs of TMPTA and MA at different functionalities.

strength and reverse impact resistance tests were performed on the low and high intensity cured coatings as listed in Table V. Lower intensity cured films showed higher fracture toughness and impact resistance while tensile strength did not show a discernable trend. Low intensity cured coatings had distinctively smaller crosslink densities at 35% TMPTA concentration. However, the low UV-intensity formed films utilizing 20% TMPTA (M0.5F3T20-2) exhibited a similar crosslink density compared to the high intensity cured film (M0.5F3T20).

The extent of microgel formation decrease in crosslink density, and hence phase separation affect the physical performance of the resin system. Fracture toughness, tensile strength and reverse impact resistance test were performed to elucidate the balance of mechanical properties. The experimental data were analyzed to fit into a reduced two factor interaction model. It was found out that there is a relationship between tensile strength and concentrations of TMP, TMPTA, and MA. Best fit model equation for tensile strength in terms of actual factors was:

$$\text{Tensile strength (MPa)} = -2.925 + 0.6000 \times \text{TMP} + 1.100 \times \text{MA} + 0.3994 \times \text{TMPTA} - 0.0052 \times \text{TMPTA}^2 \quad (3)$$

The model F-value tests the significance of adding nonlinear terms to the model. A model F-value of 22.2 implied that the model was significant. There was only 0.01% chance that a model F-value this large could occur due to noise. ''Prob > F'' values less than 0.05 indicate model terms are significant. In this model, TMP, MA, TMPTA, and TMPTA^2 were the significant terms. The lack of fit F-value of 3.56 implied non-significant lack of fit. The model adequate precision ratio of 15.6 indicated an adequate signal. Therefore, this model was used to navigate the design space. Figure 10, demonstrates 3D design expert response surface plot of the model predicted for the tensile strength of the films.

Tensile strength was first increased with the increase in TMPTA concentration and, then decreased (see Fig. 9). Decrease in tensile strength can be attributed to the high amount of microgel formation and hence extent of phase separation at high reactive diluent concentrations. Replacing higher amounts of ADA with MA produced higher tensile strength films possibly due to the increase in the rigidity of the main polyester chain. Increase of the acrylate functionality of the polyesters slightly increased the tensile strength.

The fracture toughness (K_c) is a measure of resistance to crack extension. The response function equation obtained for K_c of the films in terms of actual factors was a reduced quadratic model:

$$[K_c(\text{MPam}^{1/2})]^{-1} = 0.0604 - 0.0133 \times \text{TMP} - 0.0440 \times \text{MA} - 0.0008 \times \text{TMPTA} + 0.0146 \times \text{TMP} \times \text{MA} + 0.0006 \times \text{MA} \times \text{TMPTA} \quad (4)$$

The model F-value of 156 suggested that the model was significant. A model F-value this large could occur due to noise with just 0.01% chance. The

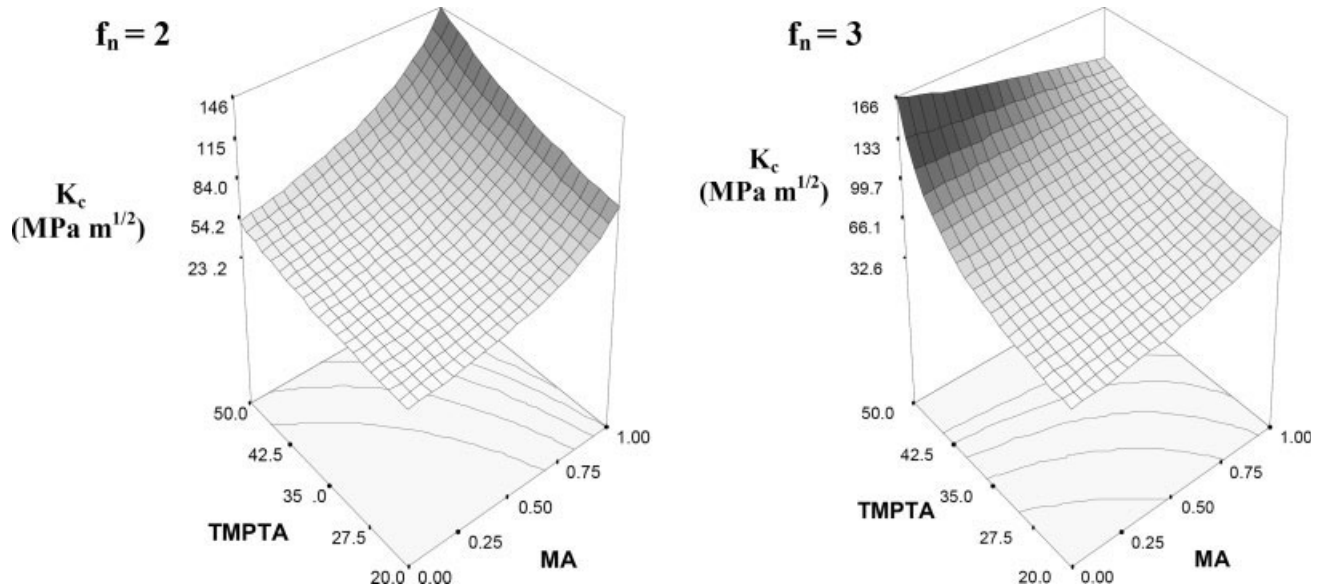

Figure 11 Fracture-Toughness: response surface graphs of the films.

lack of fit F-value of 1.55 indicated nonsignificant lack of fit relative to the pure error. To fit the model a nonsignificant lack of fit was needed. The model adequate precision ratio of 40.2 indicated that there was an adequate signal. Therefore, this model could be used to navigate the design space.

Figure 11 illustrates prediction of 3D fracture toughness (K_c) response surface graphs of films made through polyesters with acrylate functionalities 2 and 3. Fracture toughness is a very complex behavior. A coating film may not resist crack propagation under certain load whereas, it can withstand the same tensile load in its intact form. Increase in the extent of internal unsaturation at lower acrylate functionality produced higher K_c. However, at higher acrylate functionality and reactive diluent concentrations, K_c exhibited an inversely proportional behavior. This may be due to the extent of phase separation in films containing high concentrations of reactive monomer and highly unsaturated polyesters. One may expect a decrease in fracture toughness behavior due to the decrease in crosslink density, and hence stiffness. However, this was not the case, i.e. fluctuations in crosslink density due to the extent of trapped radical did not affect the fracture toughness behavior. Microgel may function as reinforcement against crack propagation and hence compensates effect of crosslink density decrease. Therefore, it can be concluded that microgel formation does not affect the overall fracture toughness unless it causes phase separation. Optimum fracture toughness values can be only obtained restricting phase separation while favoring microgel formation.

The reverse impact resistance experimental data were analyzed and fitted into a reduced quadratic model expressed by the equation below in actual factors:

$$\begin{aligned}\text{Reverse impact resistance (kg/cm)} &= 67.76 - 4.500 \times \text{TMP} + 30.85 \times \text{MA} - 2.650 \\ &\times \text{TMPTA} - 24.79 \times \text{MA}^2 + 0.0297 \times \text{TMPTA}^2 \quad (5)\end{aligned}$$

The model F-value of 15.5 indicated the model was significant. There was only 0.04% chance that a model F-value this large could occur due to noise. The lack of fit F-value of 1.54 implied a nonsignificant lack of fit compared with the experimental error. The model adequate precision ratio of 12.4 indicated that there was an adequate signal. Therefore, this model was a suitable model used to for the design space.

Figure 12 depicts the 3D reverse impact resistance response surfaces at 35% TMPTA and 2.5 acrylate functionality. Reverse impact resistance was extensively effected by the change in the internal unsaturation content. Microgels may function as micro-support units and increase the impact resistance of the films (see Fig. 11). All of the lower UV intensity cured films showed β-transitions below -50°C (see Figs. 7–9). Detection of a β-transition can be an indication of high extent of microgel formation. It has been earlier suggested that there is a correlation between impact resistance and occurrence of β-transitions; i.e. high impact resistance polymers typically undergoes a β-relaxation.[30] Lower intensity cured films having higher fracture toughness values also showed β-transitions. Therefore, it can be suggested

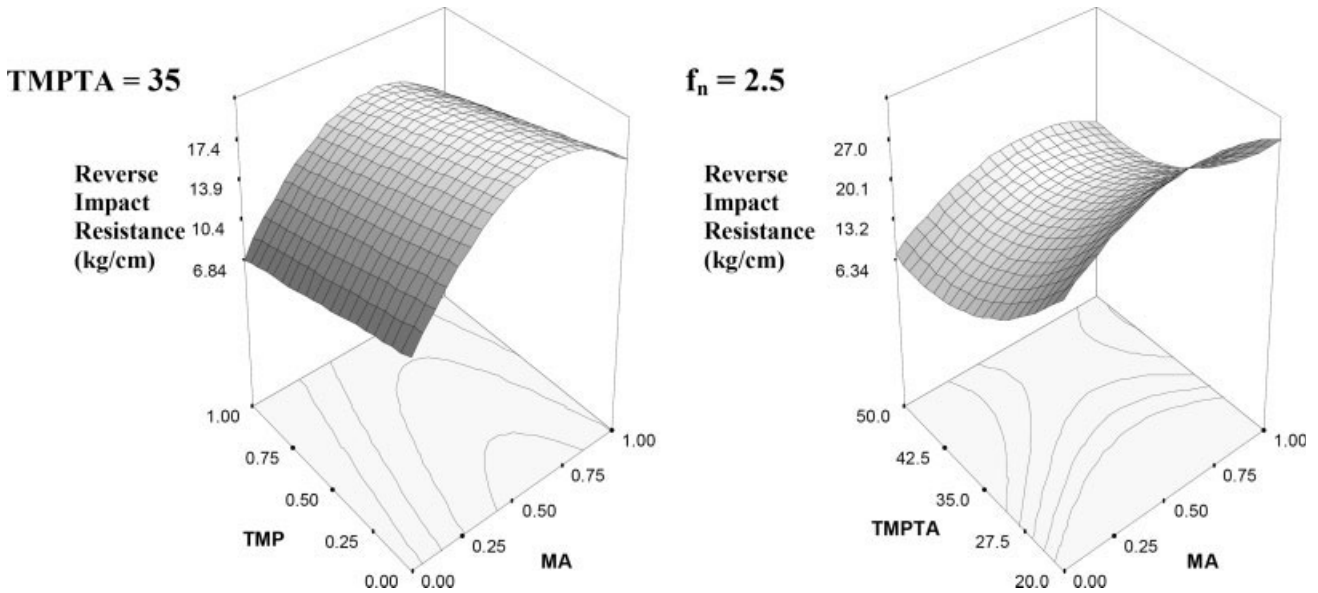

Figure 12 Reverse impact resistance 3D response surface graphs.

that there is a relation between fracture toughness and main chain secondary loss processes.

Network characterization and structure–property relationships in UV-cured UPE acrylate films were not previously reported in the literature. In this study, complex, nonlinear relationships in UV-curing UPE acrylate coatings were successfully revealed via utilizing response surface methodology. Phase separation and formation of microgel particles during network formation was suggested to describe abnormal viscoelastic and mechanical properties. It was proposed that microgel formation does not cause inferior mechanical properties, but the phase separation does. Therefore, it is essential to control the extent of microgelation and minimize the phase separation to optimize the film properties.

CONCLUSION

Effect of the multiacrylate functional reactive diluent, degree of internal unsaturation, and functionality of the polyester acrylates on viscoelastic properties, fracture toughness, tensile strength, and reverse impact resistance were investigated. Formation of microgel particles due to the cyclization reactions early in the network formation was attributed to certain viscoelastic and mechanical properties. It is essential to control phase separation and microgel formation to obtain optimum mechanical properties. It was proposed that microgels function as support units and improve fracture toughness and impact resistance. Also, a relationship was proposed between microgel formation and secondary relaxations along with the relationships between fracture toughness, impact resistance and appearance of β-transitions. Detection of β-relaxations indicates higher microgel content and, hence higher impact resistance and fracture toughness values.

References

1. Chiocchetti, P. Polym Paint Col J 1988, 178, 4216.
2. Roffey, G. C. Photopolymerization of Surface Coatings; Wiley: New York, 1982.
3. Webster, G. Chemistry and Technology of UV and EB Formulation for Coatings, Inks and Paints: Prepolymers and Reactive Dilutents for UV and EB Curable Formulations; Wiley: New York, 1997.
4. Mehnert, R.; Pincus, A.; Janorsky, I.; Stowe, R.; Berejka, A. Chemistry and Technology of UV and EB Formulations for Coatings, Inks, and Paints: UV and EB Curing Technology and Equipment; Wiley: New York, 1998.
5. Cook, D. W.; Lau, M.; Mehrabi, M.; Dean, K.; Zipper, M. Polym Int 2001, 50, 129.
6. Wicks, Z. W.; Jones, F. N.; Pappas, S. P. Organic Coatings Science and Technology, 2nd ed.; Wiley: New York, 1999.
7. Kloosterboer, J. G. Adv Polym Sci 1988, 84, 1.
8. Hild, G.; Okasha, R. Macromol Chem 1985, 186, 389.
9. Muzumdar, S. V.; Lee, L. J. Polym Eng Sci 1991, 31, 1647.
10. Liu, S. B.; Yu, T. L. Macromol Chem Phys 1995, 196, 1307.
11. Yang, Y. S.; Suspene, L. Polym Eng Sci 1991, 31, 321.
12. Chen, J. S.; Yu, T. L. J Appl Polym Sci 1997, 69, 871.
13. Brill, R. P.; Palmese, G. R. J Appl Polym Sci 2000, 76, 1572.
14. Simon, G. P.; Allen, P. E. M.; Williams, D. R. G. Polymer 1991, 32, 2577.
15. Young, J. S.; Bowman, C. N. Macromol 1999, 32, 6073.
16. Djonlagic, J.; Zlatanic, A. Macromol Chem Phys 1997, 198, 1775.
17. Djonlagic, J.; Zlatanic, A.; Dunjic, B.; Macromol Chem Phys 1998, 199, 2029.
18. Zlatanic, A.; Dunjic, B.; Djonlagic, J. Macromol Chem Phys 1999, 200, 2048.

19. Peinado, C.; Alonso, A.; Salvador, E. F.; Baselga, J.; Catalina, F. Polymer 2002, 43, 5355.
20. Kannurpatti, A. R.; Anseth, J. W.; Bowman, C. N. Polymer 1998, 39, 2507.
21. Yu, Q.; Nauman, S.; Santree, J. P.; Zhu, S. J Appl Polym Sci 2001, 82, 1107.
22. Barbeau, P.; Gerard, J. F.; Pascault, J. P.; Vigier, G. J Polym Sci Part B: Polym Phys 1999, 37, 919.
23. Myers, R. H.; Montgomery, D. C. Response Surface Methodology, Process and Product Optimization Using Designed Experiments; Wiley: New York, 2002.
24. Araujo, O.; Reinaldo, G.; Saldivar, E. J Appl Polym Sci 2001, 79, 2360.
25. Boenig, H. V. Unsaturated Polyesters: Structure and Properties; Elsevier: New York, 1964.
26. Williams, J. G. Fracture Mechanics of Polymers; Wiley: New York, 1987.
27. Ballard, R. L.; Sailer, R. A.; Larson, B.; Soucek, M. D. J Coat Tech 2001, 73, 107.
28. Jordens, K.; Wilkes, G. J Macromol Sci Chem 2001, A38, 185.
29. Yang, Y. S.; Lee, L. J. Polymer 1988, 29, 1793.
30. Allen, P. E. M.; Simon, G. P.; Williams, D. R. G.; Williams, E. H. Macromolecule 1989, 22, 809.
31. Fried, J. R. Physical Properties of Polymers Handbook; AIP Press: New York, 1996.